Measurement of the CKM angle γ in $B^{\pm} \to DK^{\pm}$ decays with the BABAR detector: status and prospects

Nicola Neri[1] [a]

INFN Pisa, Largo B. Pontecorvo, 3 56127 Pisa Italy

Abstract. We report on the measurement of the CKM angle γ in $B^{\pm} \to DK^{\pm}$ decays with the BABAR detector. A general overview of different methods of analysis and a critical discussion of the most sensitive methods are presented here.

PACS. 13.25.Hw Decays of bottom mesons – 11.30.Er Charge conjugation, parity, time reversal, and other discrete symmetries – 13.90.+i Other topics in specific reactions and phenomenology of elementary particles

1 Introduction

CP violation (CPV) was first established in $K_L \to \pi^+\pi^-$ decays in 1964 [1]. It has been accomodated in the Standard Model (SM) by a CP-violating phase in the matrix that describes the mixing of the quarks under the weak interaction, known as the CKM matrix [2]. The unitarity constraints of the CKM matrix gives us $V_{ud}V_{ub}^* + V_{cd}V_{cb}^* + V_{td}V_{tb}^* = 0$, the so-called Unitarity Triangle relation, represented in Fig. 1. CPV is proportional to the area of the triangle and requires that the angles and sides are different from zero. The primary goal of the B-factories is the study
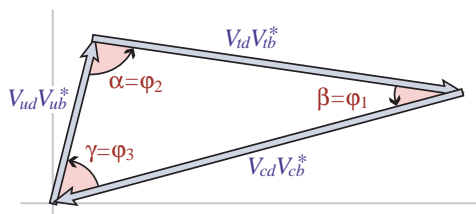

Fig. 1. Graphical representation of the unitarity constraint $V_{ud}V_{ub}^* + V_{cd}V_{cb}^* + V_{td}V_{tb}^* = 0$ as a triangle in the complex plane.

of CP violation in the B_d and B_u meson system. Overcontraining of the Unitarity Triangle parameters, measuring the sides and the angles of the triangle, represents one of the most stringent tests of the SM. The precise measurement of the angle $\gamma \equiv \arg(-V_{ud}V_{ub}^*/V_{cd}V_{cb}^*)$ is a crucial goal for this scientific program, yet it is also one of the most difficult to achieve.

[a] on behalf of the BABAR collaboration.

2 General overview of the methods

There are several decay modes that can be used to measure the angle γ, each with its own merits and drawbacks.

In $B^{\pm} \to DK^{\pm}$ decays[1], if we consider the decay modes of the neutral D meson that are accessible to both D^0 and $\bar{D}^0$, we can reach the final state through two different quark-level processes, as shown in Fig.2. The interference between the two quark-level processes $b \to u\bar{c}s$ and $b \to c\bar{u}s$ (respectively $B^- \to D^0K^-$ and $B^- \to \bar{D}^0K^-$) introduces a relative phase γ in the decay amplitude.

By neglecting the $D^0-\bar{D}^0$ mixing [3], it is possible to determine the angle γ without hadronic uncertainties, since the main contributions to the decay amplitude come from tree-level transitions. Several decay modes can be

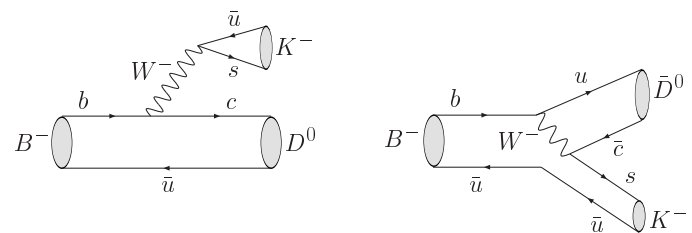**Fig. 2.** Main diagrams contributing to $B^{\pm} \to DK^{\pm}$ decay. The left diagram proceeds via V_{cb} transition, while the right diagram proceeds via V_{ub} transition and is color suppressed.

studied, including $B^{\pm} \to DK^{\pm}$, $B^- \to D^*K^-$ and $B^- \to DK^{*-}$, which have the same quark-level process in common. In the following, whenever we write $B^{\pm} \to D^{(*)}K^{(*)\pm}$

[1] In what follows, the symbol D refers to either D^0 or $\bar{D}^0$.

we intend all the above-mentioned decay modes, unless explicitly stated. Three different analysis methods have been used so far:

- GLW method [4]: where the D is recontructed in CP eigenstates (D^0_{CP}) decay modes.
- ADS method [5]: with D reconstructed in doubly Cabibbo suppressed decay modes.
- Dalitz method [6]: where the D is reconstructed in 3-body final states and the angle γ is extracted through an analysis of the distribution of the events in the D Dalitz plane [7].

The sensitivity of the different methods to γ depends on the magnitude of the ratio

$$r_B = \left| \frac{A(b \to u\bar{c}s)}{A(b \to c\bar{u}s)} \right|$$

of the $b \to u\bar{c}s$ amplitude with respect to the $b \to c\bar{u}s$ one. The value of r_B is a key quantity which has a significant impact on the ability to measure the CKM angle γ at the B-factories and beyond. Note that r_B takes different values for different B decays. Theoretical expectations for r_B are in the range $\approx 0.1 - 0.2$ [4,8], in agreement with the 90% C.L. upper limits on r_B set by BABAR ($r_B <$ 0.23) [9] and Belle ($r_B < 0.18$) [10] through the study of $B^- \to DK^-, D \to K^+\pi^-$ decays.

3 The GLW method: $B^\pm \to DK^\pm$ with D^0_{CP} Decays

This method considers the $B^\pm \to DK^\pm$ decays , where the D decays to a CP eigenstate. The CP observables are:

$$R_{CP\pm} \equiv \frac{\mathcal{B}\left(B^- \to D^0_{CP\pm}K^-\right) + \mathcal{B}\left(B^+ \to D^0_{CP\pm}K^+\right)}{\mathcal{B}\left(B^- \to D^0K^-\right) + \mathcal{B}\left(B^+ \to \overline{D}^0K^+\right)}$$

$$\equiv 1 + r_B{}^2 \pm 2r_B \cos\delta_B \cos\gamma$$

$$A_{CP\pm} \equiv \frac{\mathcal{B}\left(B^- \to D^0_{CP\pm}K^-\right) - \mathcal{B}\left(B^+ \to D^0_{CP\pm}K^+\right)}{\mathcal{B}\left(B^- \to D^0_{CP\pm}K^-\right) + \mathcal{B}\left(B^+ \to D^0_{CP\pm}K^+\right)}$$

$$\equiv \frac{\pm 2\, r_B \sin\delta_B \sin\gamma}{R_{CP\pm}}$$

where δ_B is the strong phase difference between the V_{ub} and the V_{cb} mediated amplitudes. Here, $D^0_{CP\pm} = (D^0 \pm \overline{D}^0)/\sqrt{2}$ are the CP eigenstates of the neutral D meson system. The main advantage of this method is that γ can be extracted in a theoretically-clean manner if one reconstructs D^0_{CP}-even and D^0_{CP}-odd decays. In fact, the number of unknowns is three (r_B, γ, δ_B) and we have three linear independent observables. However, an 8-fold ambiguity on the value of γ is not resolved since the ambiguities on $(\gamma, \delta_B) \to (\delta_B, \gamma)$ and on the sign of $\sin\gamma$, which admits four different solutions, are indistinguishable. In principle, carrying out analyses for the different decay modes of $B^\pm \to D_{CP}X^\pm$, where $X^\pm = K^\pm, K^\pm\pi^0, K^0_s\pi^\pm, (K\pi\pi)^\pm$, makes it possible to solve the ambiguity on the magnitude

of $\sin\gamma$, since each of the decay modes has the same weak phase γ but a different final-state phase difference δ_B. The event yield is similar for the CP-even and the CP-odd decay modes - almost 150 signal events with the present statistics in $B^\pm \to DK^\pm$ decay modes. Fig. 3 shows the ΔE distribution for the signal and background events of the reconstructed modes: $D^0_{CP+} \to \pi^+\pi^-, K^+K^-$, and $D^0_{CP-} \to K^0_s\pi^0, K^0_s\omega, K^0_s\phi$. Here, ΔE is the difference between the measured B meson energy and the energy of the beam in the center of mass system, and peaks near zero for signal events.

The total reconstruction efficiencies, based on simulated signal events, are 30-40% for the D^0_{CP+} modes and 10-20% for the D^0_{CP-}. Experimentally, the $R_{CP\pm}$ ratios are computed using the $R_{CP\pm} \simeq R_\pm/R$ relations, where the quantities R and $R_\pm$ are defined as:

$$R = \frac{\mathcal{B}(B^- \to D^0K^-) + \mathcal{B}(B^+ \to \overline{D}^0K^+)}{\mathcal{B}(B^- \to D^0\pi^-) + \mathcal{B}(B^+ \to \overline{D}^0\pi^+)} ,$$

$$R_\pm = \frac{\mathcal{B}(B^- \to D^0_{CP\pm}K^-) + \mathcal{B}(B^+ \to D^0_{CP\pm}K^+)}{\mathcal{B}(B^- \to D^0_{CP\pm}\pi^-) + \mathcal{B}(B^+ \to D^0_{CP\pm}\pi^+)} .$$

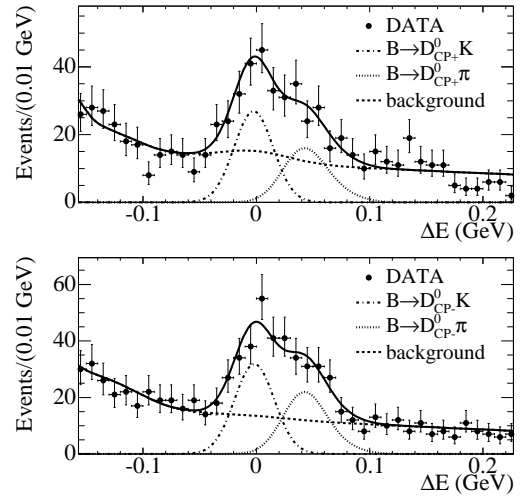Systematic uncertainties are canceled out in the measurement of these double ratios. The results for the R_{CP} and

Fig. 3. Distributions of ΔE for events enhanced in $B^- \to DK^-$ signal. Top: $B^- \to D_{CP+}K^-$; bottom: $B^- \to D_{CP-}K^-$. Solid curves represent projections of the maximum likelihood fit; dashed, dashed-dotted and dotted curves represent the $B^- \to DK^-$, $B^- \to D\pi^-$ and background contributions.

A_{CP} observables using BABAR data [11] are reported in Table 1. The precision of these measurements does not significantly constrain the value of γ, but when combined with the existing measurements of the $B^\pm \to D^{(*)}K^{(*)\pm}$ decays, it will improve the knowledge of the angle γ and of the parameter r_B.

Table 1. Measured ratios $R_{CP\pm}$ and $A_{CP\pm}$ for CP-even and CP-odd D decay modes. The first error is statistical, the second is systematic.

B mode	$N(B\overline{B}) \cdot 10^6$	R_{CP+}	A_{CP+}	R_{CP-}	A_{CP-}
$B^\pm \to DK^\pm$	232	$0.90 \pm 0.12 \pm 0.04$	$0.35 \pm 0.13 \pm 0.04$	$0.86 \pm 0.10 \pm 0.05$	$-0.06 \pm 0.13 \pm 0.04$
$B^\pm \to D^*K^\pm$	123	$1.06 \pm 0.26^{+0.10}_{-0.09}$	$-0.10 \pm 0.23^{+0.03}_{-0.03}$	-	-
$B^\pm \to DK^{*\pm}$	232	$1.96 \pm 0.40 \pm 0.11$	$-0.08 \pm 0.19 \pm 0.08$	$0.65 \pm 0.26 \pm 0.08$	$-0.26 \pm 0.40 \pm 0.12$

4 The ADS method: $B^\pm \to DK^\pm$ with Double-Cabibbo-Suppressed D Decays

In the ADS method, the favored B decay ($B^- \to D^0 K^-$) followed by the doubly CKM-suppressed D decay ($D^0 \to K^+\pi^-$) interferes with the suppressed B decay ($B^- \to \overline{D}^0 K^-$) followed by the CKM-favored D decay ($\overline{D}^0 \to K^+\pi^-$). As a result, the two interfering amplitudes become comparable. The CP asymmetry is potentially larger in these modes than in the GLW method, however the decays have a smaller branching ratio, on the order of 10^{-7}.

The observables sensitive to the CP parameters are

$$R_{ADS} \equiv \frac{\mathcal{B}\left([K^+\pi^-]_D K^-\right) + \mathcal{B}\left([K^-\pi^+]_D K^+\right)}{\mathcal{B}\left([K^-\pi^+]_D K^-\right) + \mathcal{B}\left([K^+\pi^-]_D K^+\right)}$$

$$\equiv r_B{}^2 + r_D{}^2 + 2r_B r_D \cos\gamma \cos(\delta_B + \delta_D)$$

$$A_{ADS} \equiv \frac{\mathcal{B}\left([K^+\pi^-]_D K^-\right) - \mathcal{B}\left([K^+\pi^-]_D K^+\right)}{\mathcal{B}\left([K^+\pi^-]_D K^-\right) + \mathcal{B}\left([K^+\pi^-]_D K^+\right)}$$

$$\equiv \frac{2\, r_B r_D \sin\gamma \sin(\delta_B + \delta_D)}{r_B{}^2 + r_D{}^2 + 2r_B r_D \cos\gamma \cos(\delta_B + \delta_D)}$$

where δ_D is the relative strong phase in the D^0 decay and $r_D \equiv \left|\frac{A(D^0 \to K^+\pi^-)}{A(D^0 \to K^-\pi^+)}\right|$ is the magnitude of the ratio of the amplitude of the doubly-Cabibbo-suppressed D^0 decay to that of the Cabibbo-allowed one. The value of r_D has been measured to be $r_D = 0.060 \pm 0.002$ [12].

In this method, each B decay mode has two indepedent equations (R_{ADS}, A_{ADS}) that cannot be solved for three unknowns (r_B, γ, $\delta_B + \delta_D$). In order to determine the value of γ, for a given B decay mode it is necessary to reconstruct at least two different D^0 decay modes, such as $B^- \to [K^+\pi^-]_D K^-$, $B^- \to [K^{*+}\pi^-]_D K^-$ or $B^- \to [K^+\rho^-]_D K^-$. In the case of two D^0 decay modes, it is possible to extract the value of γ up to a 16-fold ambiguity, while in the case of three D^0 decay modes there remains a 4-fold ambiguity [5].

The addition of different B decay modes is helpful to constrain the value of γ. Particularly interesting are $B^- \to D^*K^-$ decays, where the D^* is reconstructed in $D^0\pi^0$ and $D^0\gamma$. In fact, there is an effective strong phase shift of π between the two cases [13], leading to two different R^*_{ADS} expressions: [2]

$$R^*_{ADS,D\pi^0} = r_B^{*2} + r_D^2 + 2r_B^* r_D \cos\gamma \cos(\delta_B^* + \delta_D),$$

$$R^*_{ADS,D\gamma} = r_B^{*2} + r_D^2 - 2r_B^* r_D \cos\gamma \cos(\delta_B^* + \delta_D),$$

---

[2] Here and in the following the '*' symbol indicates that the specified value refers to the $B^- \to D^*K^-$ decay mode.

where $R^*_{ADS,D\pi^0}$ ($R^*_{ADS,D\gamma}$) is the charge-independent ratio for the $B^- \to D^*K^-$ with $D^{*0} \to D^0\pi^0$ ($D^{*0} \to D^0\gamma$). Hence in the case of $B^- \to D^*K^-$, it is straightforward to determine the value for r_B through the relation

$$\frac{R^*_{ADS,D\pi^0} + R^*_{ADS,D\gamma}}{2} = r_B^{*2} + r_D^2.$$

In Fig. 4 it is shown the m_{ES} distribution with fit model overlaid for candidate signal events. With the present statistics there is no evident signal in $B^\pm \to D^{(*)}K^{(*)\pm}$ decay modes at the B-factories. The experimental observables R_{ADS} have been measured in $B^\pm \to D^{(*)}K^{(*)\pm}$ decays and they were found to be consistent with zero. However, it is possible to set an upper limit to the value of r_B as shown in Fig. 5. The summary of the results is reported in Table 2.

Table 2. Measured charge-independent ratios R_{ADS} for $B^\pm \to D^{(*)}K^{(*)\pm}$ decay modes. Where a single term for the error is specified, it includes the statistical and the systematic contribution, otherwise the first error is statistical, the second is systematic. The 90% C.L. limits reported are evaluated without any assumptions for the values of γ and $\delta_B + \delta_D$. The result for $B^\pm \to DK^{*\pm}$ is obtained combining the ADS and GLW measurements.

B mode	R_{ADS}	r_B
$B^\pm \to DK^\pm$	< 0.029 90% C.L.	$r_B < 0.23$
$B^\pm \to D^*K^\pm$	< 0.023 90% C.L.	$r_B^{*2} < (0.16)^2$
$B^\pm \to DK^{*\pm}$	$0.046 \pm 0.031 \pm 0.08$	$0.28^{+0.006}_{-0.010}$

5 The Dalitz method: $B^\pm \to DK^\pm$ with a Dalitz analysis of the $D^0 \to K_S^0\pi^+\pi^-$ decay

In the previously described methods, if the relative strong phases δ_B vanish, the sensitivity to γ is significantly reduced. In general, having large interfering amplitudes with relatively strong phases enhances the sensitivity to the phase γ. The main advantage of the method [6] is that it involves the entire resonant structure of the $D^0 \to K_S^0\pi^+\pi^-$ three-body decay, with interference between doubly-Cabibbo-suppressed, Cabibbo-allowed and CP-eigenstate amplitudes all providing the sensitivity to γ. No branching ratio measurements are needed and only charged particles are involved in the final states, which results in a
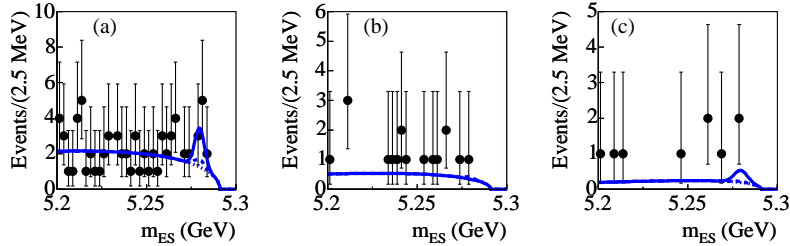
Fig. 4. m_{ES} distributions for candidate signal events with the fit model overlaid. (a) $\overline{D}K$ events. (b) $\overline{D}^*K$ events with $D^* \to D\pi^0$. (c) $\overline{D}^*K$ events with $D^* \to D\gamma$.

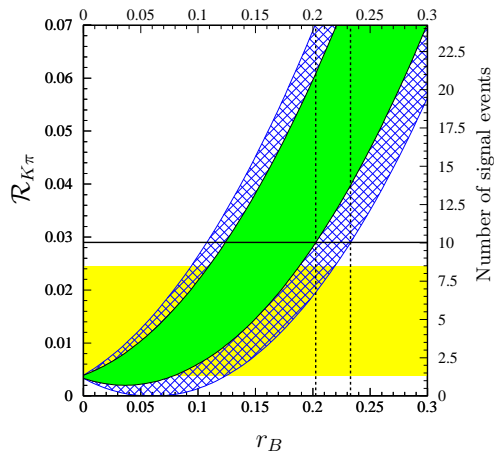**Fig. 5.** Expectations for $\mathcal{R}_{K\pi}$ and the number of signal events vs. r_B. Dark filled-in area: allowed region for any value of δ, with a $\pm 1\sigma$ variation on r_D, and $51° < \gamma < 66°$. Hatched area: additional allowed region with no constraint on γ. Note that the uncertainty on r_D has a very small effect on the size of the allowed regions. The horizontal line represents the 90% C.L. limit $\mathcal{R}_{K\pi} < 0.029$. The vertical dashed lines are drawn at $r_B = 0.203$ and $r_B = 0.233$. They represent the 90% C.L. upper limits on r_B with and without the constraint on γ. The light filled-in area represents the 68% C.L. region corresponding to $\mathcal{R}_{K\pi} = 0.013^{+0.011}_{0.009}$.

higher reconstruction efficiency and low background. The price to pay is that it requires a detailed study of the resonances and their interference through a *Dalitz plot* technique [14].

Unless otherwise stated, we use the term "Dalitz plot" to refer to the allowed kinematic region in the two-dimensional squared space m^2_- and m^2_+, where $K^0_S \pi^-$ and $K^0_S \pi^+$ m^2_- and m^2_+ are the invariant masses of $K^0_S \pi^-$ and $K^0_S \pi^+$ respectively.

Let us focus on the following cascade decay [3]

$$B^- \to DK^- \to (K_S \pi^- \pi^+)_D K^-, \qquad (1)$$

---

[3] In the following discussion we neglect $D^0 - \bar{D}^0$ mixing, which is a good approximation in the context of the Standard Model [6].

using the notation of Giri *et. al.* [6] to define the amplitudes

$$A(B^- \to D^0 K^-) \equiv A_B,$$
$$A(B^- \to \overline{D}^0 K^-) \equiv A_B r_B e^{i(\delta_B - \gamma)}. \qquad (2)$$

The same definitions apply to the amplitudes for the *CP* conjugate cascade $B^+ \to DK^+ \to (K_S \pi^+ \pi^-)_D K^+$ with the change of weak phase sign $\gamma \to -\gamma$ in (2). We have set the strong phase of A_B to zero by convention, so that δ_B is the difference of strong phases between the two amplitudes. The value of $|A_B|$ is known from the measurement of the $B^- \to D^0 K^-$ decay width using flavor specific decays of D^0. The amplitude $A(B^- \to \overline{D}^0 K^-)$ is color suppressed and cannot be determined from experiment in this way [5].

Assuming *CP* is conserved in $D^0 \to K^0_S \pi^+ \pi^-$ decay [15], we define the decay amplitude of the $A(B^- \to DK^-)$ decays, with $D^0 \to K^0_S \pi^+ \pi^-$ as

$$\mathcal{A}_D(m^2_-, m^2_+) + \kappa r_B e^{i(\delta_B - \gamma)} \mathcal{A}_D(m^2_+, m^2_-), \qquad (3)$$

where $\mathcal{A}_D(m^2_-, m^2_+)$ is the $D^0 \to K^0_S \pi^+ \pi^-$ decay amplitude. As a consequence of parity and angular momentum conservation in the $B^- \to D^* K^-$ decay, the factor κ takes the value $+1$ for $B^- \to D^* K^-$ ($D^* \to D^0 \pi^0$), and -1 for $B^- \to D^* K^-$ ($D^* \to D^0 \gamma$) [13].

A model dependent parameterization of the Dalitz structure can be introduced to reduce the number of unknown parameters to extract from the data. If the functional dependence of both the moduli and the phases of the D^0 meson decay amplitudes $A_D(m^2_-, m^2_+)$ were known, then the analysis would be simplified. There would be only three variables, $r_B, \delta_B,$ and γ, that need to be fitted. A plausible assumption, confirmed by data, is that a significant part of the three-body $D^0 \to K_S \pi^- \pi^+$ decay proceeds via two-body resonances. The $D^0 \to K^0_S \pi^- \pi^+$ decay amplitude $\mathcal{A}_D(m^2_-, m^2_+)$ hence can be determined from an unbinned maximum-likelihood fit to the Dalitz plot distribution of a D^0 sample from $D^{*+} \to D^0 \pi^+$ decays reconstructed on data.

A phenomenological model to describe $\mathcal{A}_D(m^2_-, m^2_+)$, based on Breit-Wigner (BW) parameterizations of a set of resonances, can be used. The decay amplitude of the model is then expressed as a sum of two-body decay-matrix elements (subscript r) and a non-resonant (sub-

script NR) contribution,

$$\mathcal{A}_D(m_-^2, m_+^2) = \Sigma_r a_r e^{i\phi_r} \mathcal{A}_r(m_-^2, m_+^2) + a_{\mathrm{NR}} e^{i\phi_{\mathrm{NR}}} \;, \; (4)$$

where each term is parameterized with an amplitude a_r (a_{NR}) and a phase ϕ_r (ϕ_{NR}). The function $\mathcal{A}_r(m_-^2, m_+^2)$ is the Lorentz-invariant expression for the matrix element of a D^0 meson decaying into $K_S^0 \pi^- \pi^+$ through an intermediate resonance r, parameterized as a function of position in the Dalitz plane. For $r = \rho(770)$ and $\rho(1450)$, we use the functional form suggested in Ref. [16], while the remaining resonances can be parameterized by a spin-dependent relativistic Breit-Wigner distribution [12]. An analogous phenomenological approach is represented by the K-matrix formalism [17], which provides a direct way of imposing the unitarity constraint that is not guaranteed in the case of the BW model and is suited to the study of broad and overlapping resonances in multi-channel decays. In the $D^0 \to K_S^0 \pi^+ \pi^-$ decay, the K-matrix method is suited to solve the main limitation of the Breit-Wigner model to parameterize the $\pi\pi$ S-wave states [18], thus avoiding the need to introduce the σ scalars.

The Dalitz amplitude $\mathcal{A}_D(m_-^2, m_+^2)$ can be written in this case as a sum of two-body decay matrix elements for the spin-1, spin-2 and $K\pi$ spin-0 resonances (as in the Breit-Wigner model), and the $\pi\pi$ spin-0 piece denoted as F_1 is written in terms of the K-matrix. We have

$$\mathcal{A}_D(m_-^2, m_+^2) = F_1(s) + \Sigma_{r \neq \pi\pi \, \text{S-wave}} a_r e^{i\phi_r} \mathcal{A}_r(m_-^2, m_+^2) \;,$$

where $F_1(s)$ is the contribution of $\pi\pi$ S-wave states,

$$F_1(s) = \sum_j [I - iK(s)\rho(s)]_{1j}^{-1} P_j(s) \;.$$

Here, s is the squared mass of the $\pi\pi$ system $(m_{\pi^+\pi^-}^2)$, I is the identity matrix, K is the matrix describing the S-wave scattering process, ρ is the phase-space matrix, and P is the initial production vector [19]. The index j represents the jth channel ($1 = \pi\pi$, $2 = K\overline{K}$, $3 = $ multi-meson[4], $4 = \eta\eta$, $5 = \eta\eta'$ [20]). The K-matrix parameters can be obtained from Ref. [20] from a global fit of the available $\pi\pi$ scattering data from threshold up to $1900 \, \text{MeV}/c^2$.

The BABAR analysis uses, as a "nominal" model, the isobar model, which consists of 13 resonances leading to 16 two-body decay amplitudes and phases (see Table 3), plus the non-resonant contribution.

All the resonances considered in this model are well established except for the two scalar $\pi\pi$ resonances, σ and σ', whose masses and widths are obtained from our sample. [5]

Their addition to the model is motivated by an improvement in the description of the data. The $D^0 \to K_S^0 \pi^+ \pi^-$ Dalitz distribution and the fit projections are shown in Fig. 6. The possible absence of the σ and σ' resonances is

CP parameter	$B^{\pm} \to D^{(*)}K^{\pm}$
x_-	$0.041 \pm 0.059 \pm 0.018 \pm 0.011$
y_-	$0.056 \pm 0.071 \pm 0.007 \pm 0.023$
x_+	$-0.072 \pm 0.056 \pm 0.014 \pm 0.029$
y_+	$-0.033 \pm 0.066 \pm 0.007 \pm 0.018$
x_-^*	$-0.106 \pm 0.091 \pm 0.020 \pm 0.009$
y_-^*	$-0.019 \pm 0.096 \pm 0.022 \pm 0.016$
x_+^*	$0.084 \pm 0.088 \pm 0.015 \pm 0.018$
y_+^*	$0.096 \pm 0.111 \pm 0.032 \pm 0.017$

Table 4. CP-violating parameters $x_{\mp}^{(*)}$, $y_{\mp}^{(*)}$ obtained from the CP fit to the $B^{\pm} \to D^{(*)}K^{\pm}$ samples. The first error is statistical, the second is experimental systematic uncertainty and the third is the systematic uncertainty associated with the Dalitz model.

considered in the evaluation of the systematic errors, fitting the data using the alternative K-matrix model. Once the $\mathcal{A}_D(m_-^2, m_+^2)$ amplitude is obtained from the fit on the $D^{*+} \to D^0 \pi^+$ sample, it can be fed into Eq. (3). The extraction of the angle γ is then performed through a fit to the Dalitz distribution of the D^0 in the $B^{\pm} \to DK^{\pm}$ decays. The value of the CP-odd phase γ changes sign for B^+ and B^- in Eq. (3), leading to different rates in corresponding regions of the D^0 Dalitz plane for B^+ and B^- decays. We introduce here the CP parameters $x_{\mp}$ and $y_{\mp}$ defined respectively as the real and imaginary parts of $r_B e^{i(\delta_B \mp \gamma)}$, for which the constraint $r_B{}^2 = x_{\mp}{}^2 + y_{\mp}{}^2$ holds. Experimentally, it was demonstrated that $x_{\mp}$ and $y_{\mp}$ are well-behaving fitting parameters that are unbiased with gaussian errors [21].

The results for the CP variables, using 347 million of $B\overline{B}$ events recorded with the BABAR detector, are reported in Table 4 [22]. The results of the fit are represented showing the 1σ and 2σ two-dimensional counters in Fig. 7.

A frequentist (Neyman) procedure [12,23] has been adopted to interpret the measurement of the CP parameters $(x_{\mp}^{(*)}, y_{\mp}^{(*)})$ reported in table 4 in terms of confidence regions on $\mathbf{p} = (\gamma, r_B, \delta_B, r_B^*, \delta_B^*)$. For a given $\mathbf{p}$, the five-dimensional confidence level $\mathcal{C}$ is calculated by integrating over all points in the fit parameter space closer (larger PDF) to $\mathbf{p}$ than the fitted data values. The one- (two-) standard deviation region of the CP parameters is defined as the set of $\mathbf{p}$ values for which confidence level $\mathcal{C}$ is smaller than 3.7% (45.1%). Fig. 8 shows the two-dimensional projections onto the $r_B - \gamma$ and $r_B^* - \gamma$ planes, including statistical and systematic uncertainties. The figure shows that this Dalitz analysis has a two-fold ambiguity, $(\gamma, \delta_B^{(*)}) \to (\gamma + 180^{\circ}, \delta_B^{(*)} + 180^{\circ})$, as expected from Eq. (3). From the one-dimensional projections we obtain for the weak phase $\gamma = (92 \pm 41 \pm 11 \pm 12)^{\circ}$, and for the strong phase differences $\delta_B = (118 \pm 63 \pm 19 \pm 36)^{\circ}$ and $\delta_B^* = (-62 \pm 59 \pm 18 \pm 10)^{\circ}$. No constraints on the phases are achieved at the level of two standard deviations and beyond. Similarly, for the magnitude of the ratio of decay amplitudes r_B and r_B^* we obtain the one (two) standard deviation constraints $r_B < 0.140$ ($r_B < 0.195$) and $0.017 < r_B^* < 0.203$ ($r_B^* < 0.279$). In all cases, the first
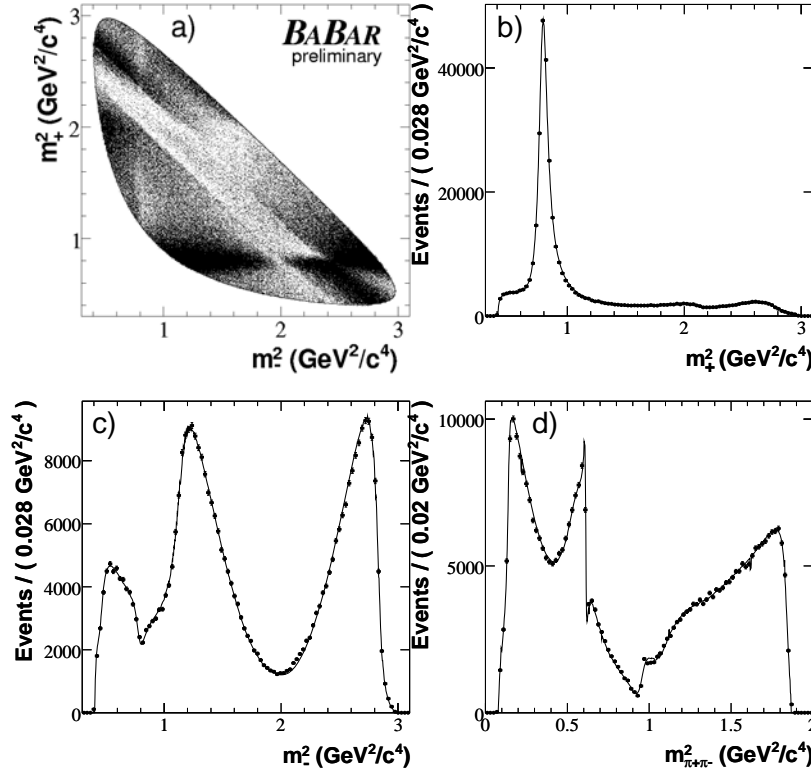
---

[4] Multi-meson channel refers to a final state with four pions.

[5] The σ and σ' masses and widths are determined from the data. We find (in MeV/c^2) $M_{\sigma} = 490 \pm 6$, $\Gamma_{\sigma} = 406 \pm 11$, $M_{\sigma'} = 1024 \pm 4$, and $\Gamma_{\sigma'} = 89 \pm 7$. Errors are statistical.

Fig. 6. (a) The $\bar{D}^0 \to K_S^0 \pi^- \pi^+$ Dalitz distribution from $D^{*-} \to \bar{D}^0 \pi^-$ events, and projections on (b) $m_+^2 = m_{K_S^0 \pi^+}^2$, (c) $m_-^2 = m_{K_S^0 \pi^-}^2$, and (d) $m_{\pi^+\pi^-}^2$. $D^0 \to K_S^0 \pi^+ \pi^-$ from $D^{*+} \to D^0 \pi^+$ events are also included. The curves are the reference model fit projections.

Component	$Re\{a_r e^{i\phi_r}\}$	$Im\{a_r e^{i\phi_r}\}$	Fit fraction (%)
$K^*(892)^-$	-1.223 ± 0.011	1.3461 ± 0.0096	58.1
$K_0^*(1430)^-$	-1.698 ± 0.022	-0.576 ± 0.024	6.7
$K_2^*(1430)^-$	-0.834 ± 0.021	0.931 ± 0.022	3.6
$K^*(1410)^-$	-0.248 ± 0.038	-0.108 ± 0.031	0.1
$K^*(1680)^-$	-1.285 ± 0.014	0.205 ± 0.013	0.6
$K^*(892)^+$	0.0997 ± 0.0036	-0.1271 ± 0.0034	0.5
$K_0^*(1430)^+$	-0.027 ± 0.016	-0.076 ± 0.017	0.0
$K_2^*(1430)^+$	0.019 ± 0.017	0.177 ± 0.018	0.1
$\rho(770)$	1	0	21.6
$\omega(782)$	-0.02194 ± 0.00099	0.03942 ± 0.00066	0.7
$f_2(1270)$	-0.699 ± 0.018	0.387 ± 0.018	2.1
$\rho(1450)$	0.253 ± 0.038	0.036 ± 0.055	0.1
Non-resonant	-0.99 ± 0.19	3.82 ± 0.13	8.5
$f_0(980)$	0.4465 ± 0.0057	0.2572 ± 0.0081	6.4
$f_0(1370)$	0.95 ± 0.11	-1.619 ± 0.011	2.0
σ	1.28 ± 0.02	0.273 ± 0.024	7.6
σ'	0.290 ± 0.010	-0.0655 ± 0.0098	0.9

Table 3. Complex amplitudes $a_r e^{i\phi_r}$ and fit fractions of the different components ($K_S \pi^-$, $K_S \pi^+$, and $\pi^+ \pi^-$ resonances) obtained from the fit of the $D^0 \to K_S^0 \pi^- \pi^+$ Dalitz distribution from $D^{*+} \to D^0 \pi^+$ events. Errors are statistical only. Masses and widths of all resonances are taken from [12] with the exception of $K_0^*(1430)^+$ taken from [24]. The fit fraction is defined for the resonance terms as the integral of $a_r^2 |\mathcal{A}_r(m_-^2, m_+^2)|^2$ over the Dalitz plane divided by the integral of $|\mathcal{A}_D(m_-^2, m_+^2)|^2$. The sum of fit fractions is 119.5%. A value different from 100% is a consequence of the interference among the amplitudes.

error is statistical, the second systematic and the third is due to the parametrization of the $D^0 \to K_S^0 \pi^+ \pi^-$ decay amplitude.
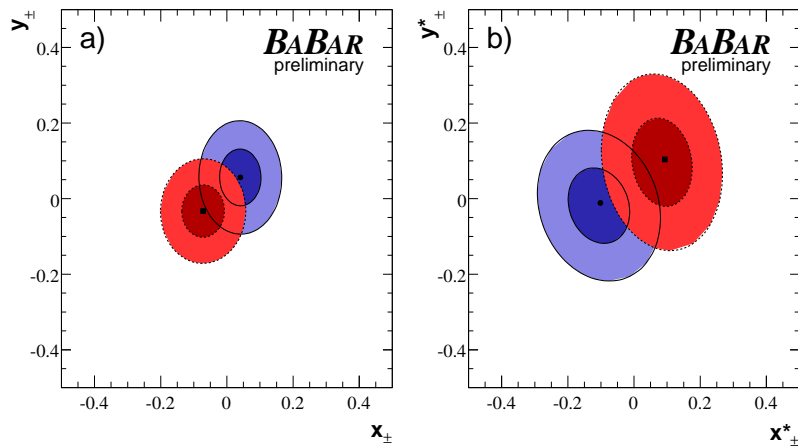
Fig. 7. Contours at 39.3% (dark) and 86.5% (light) confidence level (corresponding to two-dimensional one- and two-standard deviation regions), including statistical and systematic uncertainties, for the $(x_{\mp}^{(*)}, y_{\mp}^{(*)})$ parameters for B^- (thick and solid lines) and B^+ (thin and dotted lines) decays.
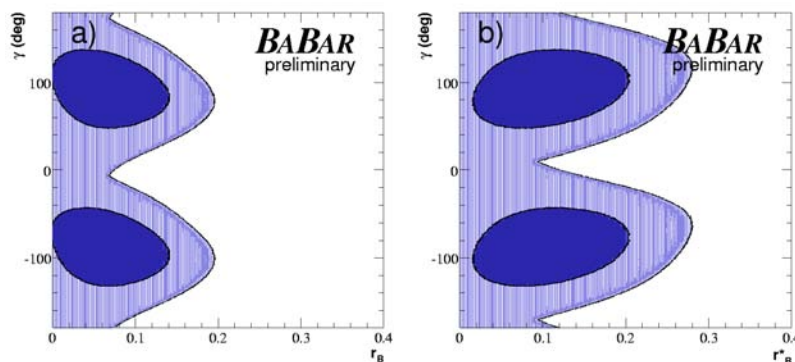

Fig. 8. Projections in the (a) $r_B - \gamma$ and (b) $r_B^* - \gamma$ planes of the five-dimensional one- (dark) and two- (light) standard deviation regions.

6 Combined measurements of γ and projections for the future

The Dalitz method has the best sensitivity to γ with the current statistics, but it is still not possible to precisely determine the value. Combining the results of several methods and different $B^{\pm} \to D^{(*)}K^{(*)\pm}$ decay modes enlarges the sensitivity to the angle γ. The measurement is dominated by statistical error, but more data will improve the precision. The projections for the measurement are highly dependent on the value of r_B, hence, it is difficult at this point to make predictions for large statistics. However, it is possible to make predictions by choosing a specific value for r_B. In Fig. 9 we show the projection for the Dalitz method and for the combined measurement of the Dalitz method, GLW and ADS, assuming $r_B = 0.1$. In this scenario, by combining different methods it will be possible to measure the angle γ with $10°$ error with a $1\ ab^{-1}$ data sample, which is within the reach of the BABAR experiment.

References

1. J. H. Christenson, J. W. Cronin, V. L. Fitch and R. Turlay,Phys. Rev. Lett. **13**, 138 (1964).
2. N. Cabibbo, *Phys. ReV. Lett.* **10**, 531 (1963);
   M. Kobayashi and T. Maskawa, *Prog. Theor. Phys.* **49**, 652 (1973).
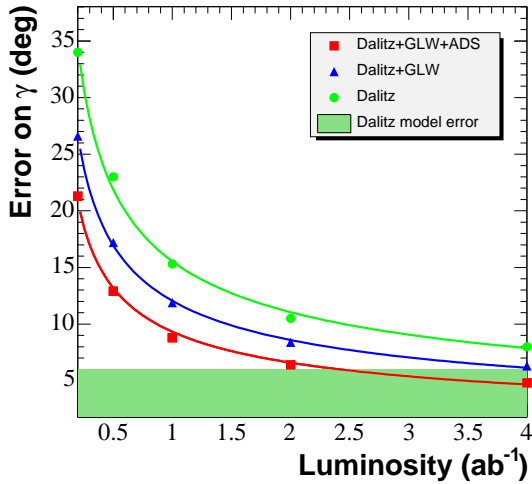3. Y. Grossman, A. Soffer, J. Zupan, Phys. Rev. **D72**, 031501 (2005).

Fig. 9. Projection of the sensitivity to γ, assuming $r_B = 0.1$, for the Dalitz method ($\bigcirc$), Dalitz + GLW combined ($\triangle$) and Dalitz + GLW + ADS combined ($\square$).The horizontal band represent the error projection due to the phenomenological parameterization of the D decay amplitude.

4. M. Gronau and D.London, *Phys. Lett.* **B253**, 483 (1991); M. Gronau and D. Wyler, *Phys. Lett.* **B265**, 172 (1991).

5. D. Atwood, I. Dunietz, and A. Soni, Phys. Rev. Lett. **78**, 3257 (1997); Phys. Rev. **D63**, 036005 (2001).

6. A. Giri, Yu. Grossman, A. Soffer and J. Zupan, *Phys. Rev. D* **68**, 054018 (2003).

7. R. H. Dalitz, *Phil. Mag.* **44**, 1068 (1953).

8. M. Gronau, Phys. Lett. **B557**, 198 (2003).

9. B. Aubert *et al.*, *Phys. Rev. D* **72**, 032004 (2005); B. Aubert *et al.*, *Phys. Rev. D* **72**, 071104 (2005)

10. M. Saigo *et al.*, Phys. Rev. Lett. **94**, 091601 (2005)

11. B. Aubert *et al.*, *Phys. Rev. Lett.* **73**, 051105 (2006); B. Aubert *et al.*, *Phys. Rev. Lett.* **72**, 071103 (2005); B. Aubert *et al.*, *Phys. Rev. D* **71**, 031102 (2005)

12. Particle Data Group, W.-M. Yao*et al.*, *J. Phys. G* **33**, 1 (2006)

13. A. Bondar and T. Gershon, Phys. Rev. **D70**, 091503 (2004).

14. Review on Dalitz plot analysis formalism in Ref. [12].

15. D. M. Asner *et al.* [CLEO Collaboration],Phys. Rev. D **70**, 091101 (2004)

16. G.J. Gounaris and J.J. Sakurai, Phys. Rev. Lett. **21**, 244, (1968).

17. E. P. Wigner, Phys. Rev. 70 (1946) 15; S. U. Chung *et al.*, Ann. Physik 4 (1995) 404.

18. Review on Scalar Mesons in Ref. [12].

19. I. J. R. Aitchison, Nucl. Phys. **A189**, 417 (1972).

20. V. V. Anisovich and A. V. Sarantev, Eur. Phys. Jour. A **16**, 229 (2003).

21. B. Aubert *et al* [BABAR Collaboration], Phys. Rev. Lett. **95**, 121802 (2005)

22. B. Aubert [BABAR Collaboration], arXiv:hep-ex/0607104.

23. J. Neyman, Phil. Trans. Royal Soc. London, Series A, **236**, 333 (1937), reprinted in *A selection of Early Statistical Papers on J. Neyman* (University of California Press, Berkeley, 1967).

24. E791 Collaboration, E. M. Aitala *et. al.*, Phys. Rev. Lett. **89**, 121801 (2002).